Sputtered nanostructured single crystalline cu doped ZnO thin films for carbon monoxide gas sensing applications

Pawan Kumar[1], Amit Sanger[2], Arvind Kumar[2], Davinder Kaur[1], Ramesh Chandra[2]*

[1]Functional Nanomaterials Research Lab, Department of Physics and Centre of Nanotechnology, Indian Institute of Technology Roorkee, Roorkee 247667, Uttarakhand, India
[2]Nanoscience Laboratory, Institute Instrumentation Centre, Indian Institute of Technology Roorkee, Roorkee 247667, India

*Corresponding author

DOI: 10.5185/amp.2018/830
www.vbripress.com/amp

Abstract

In the present work, gas sensing properties of Copper (Cu) doped Zinc Oxide (ZnO) thin films have been investigated. The nanostructured ZnO and Cu doped ZnO (CZO) thin films have been synthesized using DC magnetron sputtering on glass substrates. The effect of hydrophobicity and surface roughness of the CZO thin films on the carbon monoxide (CO) gas sensing performance have been examined. Fast response time (47 sec) and an optimum recovery time (~ 86 sec) have been witnessed at an adequate temperature of 250˚C for the samples having contact angle ~ 131º and surface roughness ~ 14.86 nm. Hydrophobicity of the surface provides short recovery time by opposing the existence of water-vapour on the surface.

Keywords: Sputtering, thin film, zinc oxide, Cu doping, hydrophobic, gas sensing.

Introduction

As we know that our atmospheric air contains the numerous kind of hazardous gases and chemical species, some of them are very harmful for human health while some of others are more or less vital in our daily life. Among all the chemical species and hazardous gases some of the gases like CO, NH_3, and H_2S are very harmful for respiratory system and are responsible for our lungs diseases up to few (25-60 ppm) levels in the environment[1-3]. Therefore, to overcome this problem many researchers have attracted their attention towards the detection of several hazardous gases at ppm level. Meanwhile in 1960, the researchers revealed that the semiconducting metal oxide materials are most promising to measure the sensing properties of the various gases present in our environment[4]. Therefore, metal oxide semiconductor based gas sensors are successfully used for monitoring the hazardous gases due to their low cost, long life time, robust and simple measurement electronics[5-7]. To enhance the sensing properties of chemiresistive gas sensors either we can chemically modified the active material by doping of noble metals or by forming the p-n heterojunction at the interface of dissimilar materials. This leads to fabrication of the new active sensing material in order to meet the remarkable high sensing performance criteria with high selectivity, fast response, low power consumption and high reproducibility and reliability[8-10]. Therefore, the chemiresistive gas sensors have attracted a notable attention of the researchers and become most enthusiastic research area among the scientific community since 1980s. Generally, the sensors are under the high demand for various field of applications such as environmental monitoring, industrial emission control, biomedical, household security and agriculture applications. In the present time, the developing nanotechnology promises incredible improvement in the sensor designing and capabilities. The main objective of this work is to fabricate the nanostructured metal oxide based CO gas sensors under low detection limit in our environment[11]. It is customary to use the several metal oxides such as TiO_2, ZnO, SnO_2, CuO, NiO and MnO_2 for CO gas sensing in the real field applications. But ZnO is the most extensively used material for sensor device applications. ZnO is n-type semiconductor with wurtzite hexagonal structure which is thermodynamically stable under the ambient conditions. This structure comprises the alternating planes (0001) with a stacking sequence of AaBbAaBb….along <0001> direction. Here, the two sublattices of wurtzite structure form the hexagonal closed packed structure that collaborate to the Zn atom is surrounding by four neighbor oxygen atoms which are situated at the edge of tetrahedron and vice versa. Furthermore, the tetrahedron includes the sp^3 covalent bonding. Moreover, ZnO depicts the six fold symmetry along the c-axis and its wurtzite structure does not possess inversion symmetry which means that crystal reveals the crystallographic polarity. Zinc oxide (ZnO) is direct band gap semiconductor which consists of the wide energy

band gap of about 3.2 eV at room temperature. It is basically n-type semiconductor material however its p-type nature is very hard to believe. The resistivity of heavily n-type doped ZnO is comparable to the indium tin oxide (ITO), which make it useful in transparent electronics. Recently, ZnO has become a potential gas sensor due to its excellent electrical properties, easy synthesis procedure and good compatibility with complementary metal oxide semiconductor (CMOS) technology[12]. Generally, the chemiresistive gas sensors are operated at high temperatures (≥350°C)[13]. Bearing in mind about the low power consumption and other operational conditions we need to fabricate the sensor which can operate at low temperatures. Therefore, many researchers have done their countless efforts to reduce the operating temperature of the gas sensors. The operating temperature may be reduced either by forming the p-n or n-n heterojunction at the interface of two dissimilar materials or by doping of other metal nanoparticles in parent oxide layer[14, 15]. M. T. Hosseinnejad et al. 2016 reported the characterization and hydrogen gas sensing performance of Al-doped ZnO thin films[16]. Herein, the operating temperature was found to be 300°C which is less than the pure ZnO sensor. Y J Li et al. 2012 synthesized the Co doped ZnO nanorods using electrodeposition method and examine their ethanol and CO gas sensing applications[17]. H. Gong et al. 2006 synthesized the Cu doped ZnO thin films for CO gas sensing applications[18]. Herein, the operating temperature was found to be 350°C with a sensor response of 5.2 for 300 ppm CO gas. Shukla et al. 2015 synthesized Cu doped ZnO thin films for CO_2 gas sensing applications[19]. Herein, the sensor response was found to be maximum at 200°C for 500-4000 ppm CO_2 gas. Here, in the present work we are reporting the single crystalline CZO nanostructured thin films for remarkable sensitive CO gas sensor. The advantage of these single crystalline n-type semiconducting metal oxides over polycrystalline is the improvement in the gas selectivity of the material towards a particular gas.

Experimental

ZnO and CZO thin films were deposited on cleaned (using acetone and isopropyl and dried in N_2 gas) glass substrates using DC magnetron reactive sputtering technique in a custom made chamber (Excel instruments) using Cu and Zn target (99.97% pure, 2" diameter and 5 mm thick). Initially, the sputtering chamber was evacuated to $2.5x10^{-6}$ torr using a turbo molecular pump backed by a rotary pump. Thereafter, high purity inert gas Ar (99.99%) and reactive gas O_2 (99.99%) were introduced separately into chamber. The target was pre-sputtered for 5 min in inert gas (Ar) to remove surface contamination. The sputtering parameters for the deposition of ZnO and CZO thin films are shown in **Table 1**.

Table 1. Sputtering parameters for CZO thin films.

Synthesis Parameters	
Targets	Zn, Cu
Base Pressure	2.5×10^{-6} Torr
Ar:O_2	2:1
Working Pressure	15 mTorr
Power	60 W (ZnO), 2.5-10 W (Cu)
Temperature	Room Temperature
Distance	6.5 cm
Time	30 min.

Characterizations

The structural analysis of samples was carried out using X-ray diffractometer (Bruker D8 advance) with CuK_α (40 KV, 20 mA) radiation. The morphologies, thickness and chemical compositions were analyzed using FE-SEM (Carl Zeiss, Ultra Plus), EDAX (Oxford Instruments), and AFM (NT-MDT Ntegra). The contact angles measurements were done using contact angle goniometry (Kruss DSA 100 easy drop). The sensing setup is described elsewhere[20]. The gas sensing measurements were carried out in-situ by two probe technique using source meter (Keithley 2400) and Nano voltmeter (Keithley 2182 A).

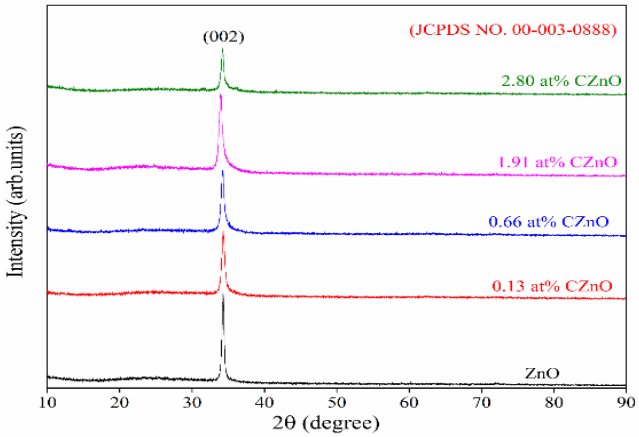

Fig. 1. XRD spectra of ZnO and CZO with various copper doping atomic percentage (0.13-2.80 at.%) thin films.

Results and discussion

Fig. 1 presents the XRD patterns of the nanostructured ZnO and CZO thin films. The dominant single crystalline peak was obtained at 34.25° attributed to (002) plane of hexagonal wurtzite phase (JCPDS 00-003-0888), which is considered as the most stable phase for ZnO at room temperature. The intensity of dominant peak varies with Cu doping percentage with a slight shift in the angle. The reason may be attributed to the plane expansion during Cu doping and that leads to loose packing structure as observed in FE-SEM images. The advantage of these single crystalline n-type semiconducting metal oxides

over polycrystalline is the improvement in the gas selectivity of the material towards a particular gas[21].

Figs. 2a-e and **3a-e** show the FE-SEM images and their corresponding cross-sectional views of ZnO and CZO thin films. We observed that all the samples consist of evenly distributed grain together with the dense, smooth and crack free surfaces. The surface microstructure of all the thin films reveal that as the Cu concentration increases from 0.13 at.% up to 1.91 at.%, the grain size reduces which is consistent with the XRD results of the thin film samples. From cross sectional view, we found that as the Cu concentration increases the thickness of the film increases from 345 nm to 560 nm. **Fig. 4a-b** shows the elemental mapping and EDAX of the ZnO thin films. We observed that all the elements are uniformly distributed over the whole surface in ZnO thin films. The EDX measurements show that ZnO layer contain about 51.49 at.% O, and 48.51 at.% Zn. **Figs 5a-b** shows the elemental mapping and EDAX of the CZO thin films. We observed that all the elements are uniformly distributed over the whole surface in CZO thin films. The EDX measurements show that CZO layer contain about 63 at.% O, 35.09 at.% Zn, and 1.91 at.% Cu.

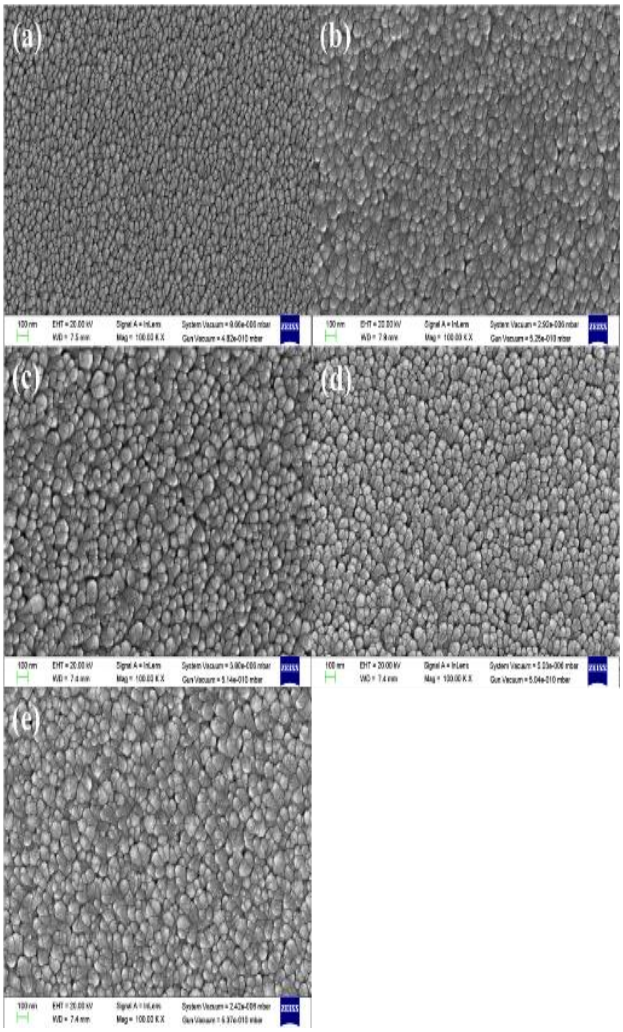

Fig. 2. SEM images of (a) ZnO, (b) 0.13 at.% CZO, (c) 0.66 at.% CZO, (d) 1.91 at.% CZO, and (e) 2.80 at.% CZO thin films.

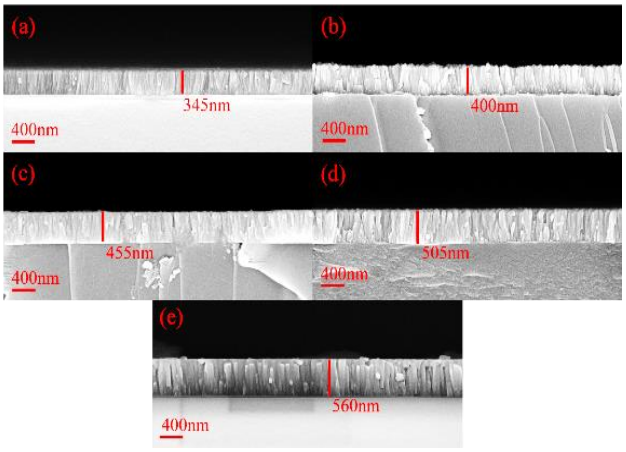

Fig. 3. SEM cross section images of (a) ZnO, (b) 0.13 at.% CZO, (c) 0.66 at.% CZO, (d) 1.91 at.% CZO, and (e) 2.80 at.% CZO thin films.

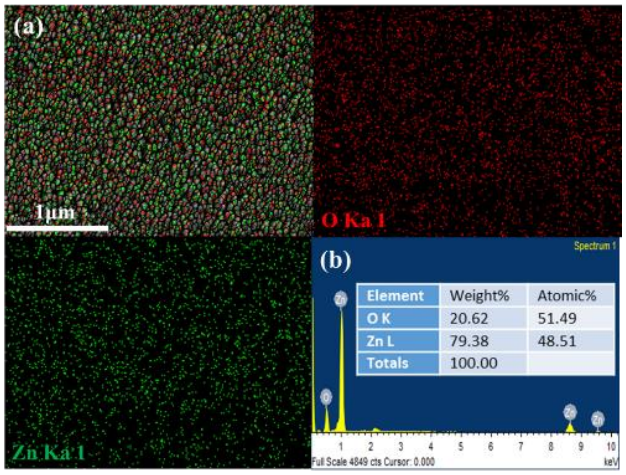

Fig. 4. (a) Elemental mapping and corresponding (b) EDAX data of ZnO thin films.

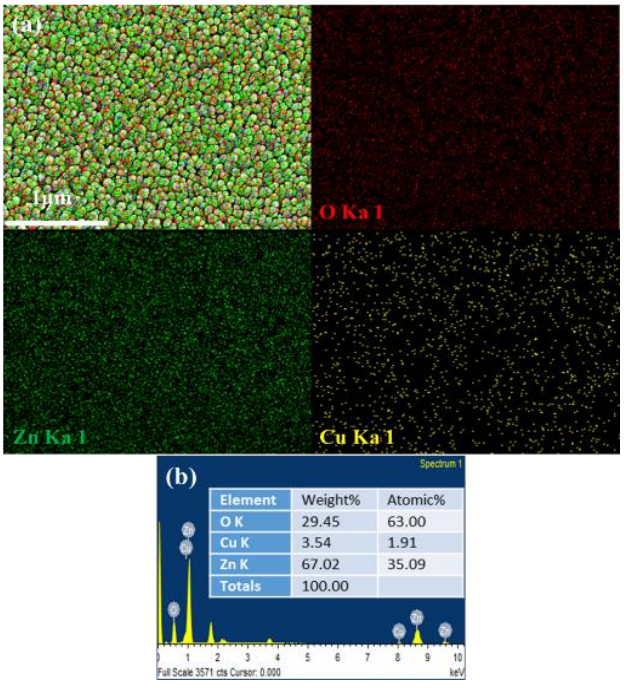

Fig. 5. (a) Elemental mapping and corresponding (b) EDAX data of 1.91 at.% CZO thin films.

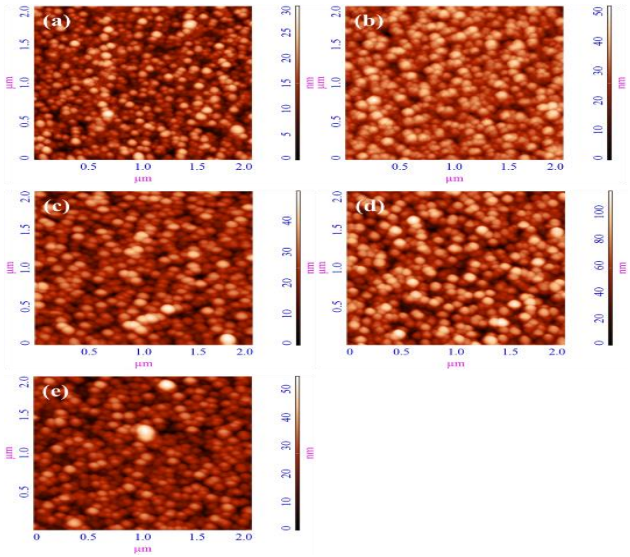

Fig. 6. 2D AFM images of (a) ZnO, (b) 0.13 at.% CZO, (c) 0.66 at.% CZO, (d) 1.91 at.% CZO, and (e) 2.80 at.% CZO thin films.

Fig. 6 and **Fig. 7** show the 2D and 3D AFM micrographs of ZnO and CZO thin films, respectively. The 2D images are complementary to the corresponding SEM images. The surface roughness of these films were found to be 4.41, 6.79, 8.14, 14.28, and 6.86 nm. It can be demonstrated that the grains are uniformly distributed over the surface and exhibits the cracks free microstructure surfaces. The average grain size of these films decreases with increasing the Cu concentration in ZnO films and then decreases at maximum doping concentration which is again consistent with the XRD results. **Fig. 8** shows the contact angle images of the ZnO and CZO thin films. The ZnO thin film shows the contact angle of 110°, while the CZO thin films have higher contact angle of 114°-128°. The CZO thin film with 1.91 at.% Cu doping shows the highest contact angle of 131°. The surface energy of these samples was found to be 8.06, 6.55, 5.55, 2.20, and 2.75 mN/m, respectively, which was determined by using two liquids (water and diiodomethane) and calculated by Owens and Wendt methods[22]. The surface roughness and contact angle images follow the Wenzel rule, justifying the increased roughness with the corresponding contact angles[7].

The sensing response of the CZO sensor exposed to 200 ppm CO in dry air at 250°C as the function of various Cu doping is plotted in Figure 9a. The sensor response was calculated as (R_a/R_g), where R_a is the response in dry air and R_g is the response in the particular gas[14]. It can be seen that the gas sensor exhibits pronounced increase in response with increasing the Cu doping about 1.91 at.%. The sensing response characteristics of ZnO and CZO thin film sensor exposed to 200 ppm CO in dry air as a function of operating temperature is shown in **Fig. 9b.** The sensing tests were performed at different operating temperatures between 50 and 300°C. These result shows that the sensor response increases with rising the operating temperature up to a critical temperature which is called the working temperature of

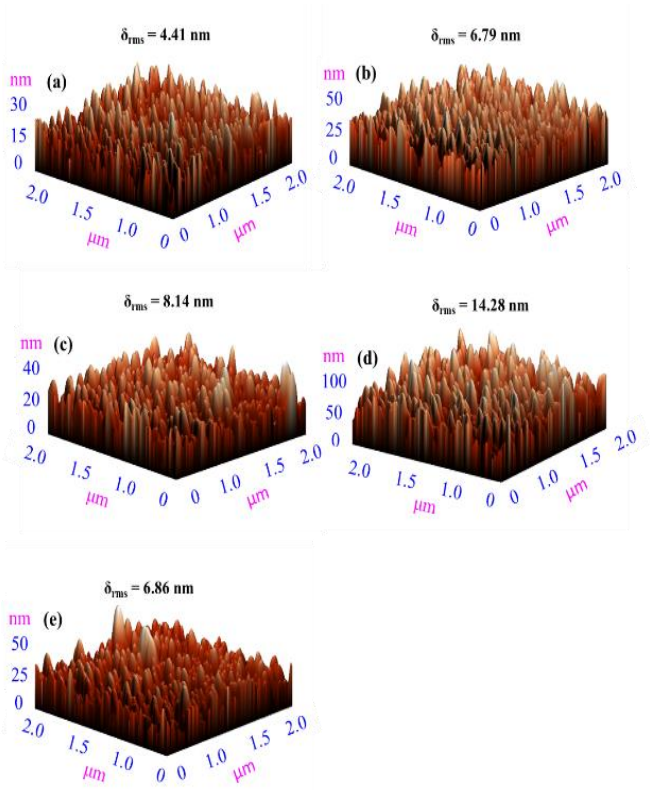

Fig. 7. 3D AFM images of (a) ZnO, (b) 0.13 at.% CZO, (c) 0.66 at.% CZO, (d) 1.91 at.% CZO, and (e) 2.80 at.% CZO thin films.

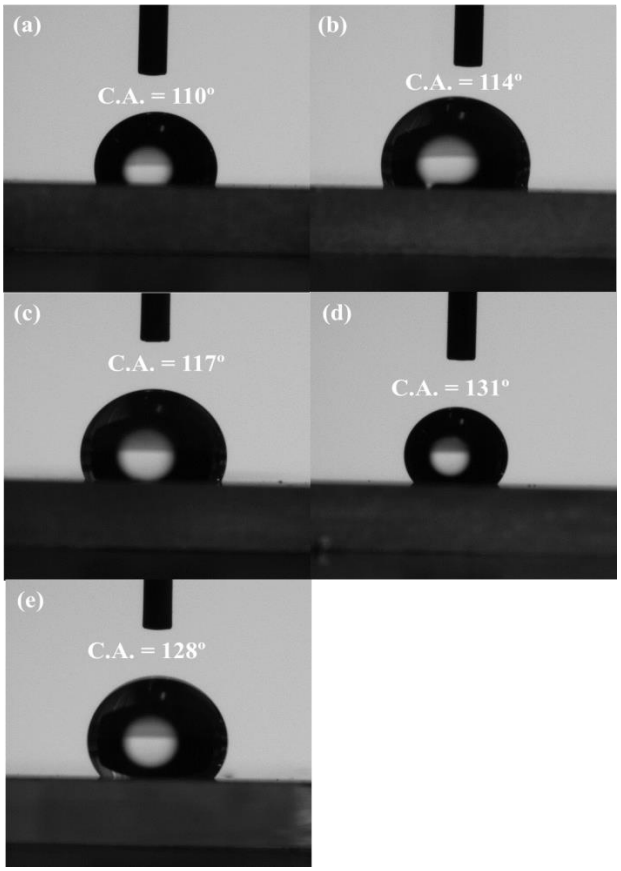

Fig. 8. Contact angle images of (a) ZnO, (b) 0.13 at.% CZO, (c) 0.66 at.% CZO, (d) 1.91 at.% CZO, and (e) 2.80 at.% CZO thin films.

the respective sensor[4, 23]. As the working temperature further increases beyond the critical value, the sensing response starts to decrease. This behavior of the sensor response with the operating temperature occurs due to slow chemical activation process between the target (CO) gas molecules and chemisorbed oxygen species reside on the surface at low working temperatures. However, at high operating temperatures the adsorbed CO gas molecules may fly off before the chemical reaction takes place on the sensor surface and thus the response starts to decrease as well[24]. Here, we observed that the operating temperature of the 1.91 at.% CZO is lower than that of pure ZnO sensor and also display greater response as compared to pure ZnO through the whole temperature region. It may be due to increasing the charge carriers at the interface and hence obvious increase the sensor response. Moreover, 1.91 at.% CZO film shows the smallest crystallite size, leading to the improvement in the sensor response. It may be expected that the proper substitution of Cu decreases the crystallite size. Here, Cu works as viaduct in case of flow of electrons which may improves the sensing characteristic of CZO thin film. Therefore, we conclude that the maximum response for 1.91 at.% CZO sensor was found at 250°C whereas the extreme response for pure ZnO sensor was observed at 300°C and it may able to detect the trace amount down to 50 ppm of CO gas. **Fig. 9c** implies the variation in the response for 1.91 at% CZO at several concentrations of CO from 50 to 1000 ppm in dry air at working temperature of 250°C. Here, as the target gas concentration increases the response enhances. For 1.91 at% of CZO gas sensor, the high response (R_a/R_g~2.76) with fast response and recovery time of 47 and 86 seconds was observed at 200 ppm level. It is predictable that the gas response is calculated by the interaction between the target gas molecules and the surface of the material. **Fig. 9d** shows the response/recovery time behavior upon exposure to several CO concentrations from 50–1000 ppm at 250°C. The fast response and recovery time were found to be 47 sec and 86 sec, respectively for 1.91 at% CZO sensor towards 200 ppm CO gas at operating temperature of 250°C. Moreover, the cross sensitivity test for 1.91 at.% CZO sensor at 250°C was studied in detail. **Fig. 9e** depicts the response curves for the CZO gas sensor at 200 ppm level upon exposure CO, NH_3, and H_2 gases mixed with dry air gas at 250°C. From these investigations, we observed that CZO sensor displays high sensitivity and selectivity towards CO gas with respect to other interfering gases. It gives quite improved results than the earlier reports for CO sensing using ZnO thin films. **Fig. 9f** shows the stability test of Cu doped ZnO gas sensor was carried out for 200 ppm CO at 250°C. It demonstrates that the CZO sensor exhibits about 5% changes in response after 60 days which collaborates the remarkable long term stability of the CZO sensor. These results reveal that the CO gas sensing properties for CZO sensor were found to be noticeably enhanced. In **Fig. 9g,** the I–V characteristics of the pure ZnO and CZO sensor exhibit the rectifying diode behavior at 250ºC. During CO exposure, the conductance of the sensor increases due to the increase in free charge carriers (i.e. electrons).

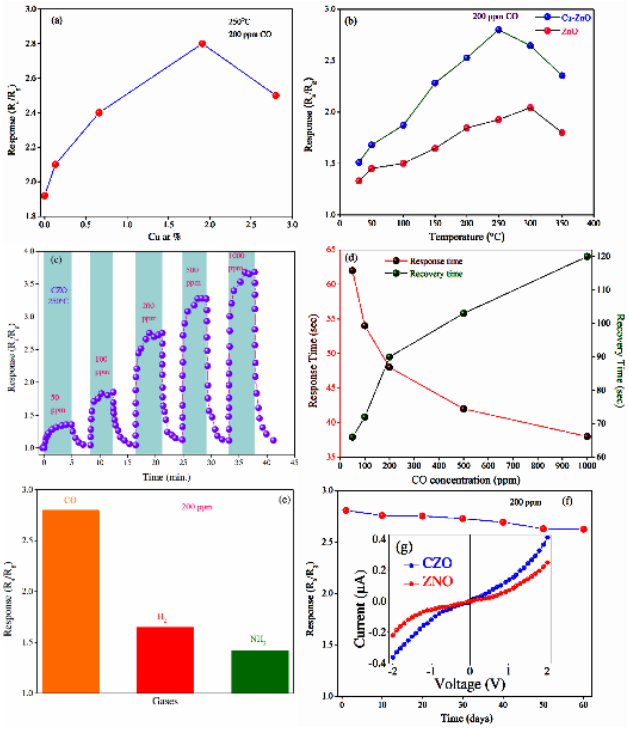

Fig. 9. (a) Gas response curve of the CZO thin film sensor as a function of Cu doping at 250°C in 200 ppm CO gas in dry air, (b) Gas response curve of the ZnO and CZO thin film sensors as a function temperature in 200 ppm CO gas in dry air, (c) Gas response curve of CZO thin film sensor as a function of the CO gas concentration (50–1000 ppm in dry air) at 250°C, (d) Response and recovery time versus CO gas concentrations in dry air, (e) Gas selectivity curves of the CZO thin film sensor to 200 ppm of different gases at 250°C, (f) Response time behavior for 90 days, implying the superior long-term stability of the sensor, and (g) I–V characteristics of the CZO thin film sensor before and after CO gas (200 ppm) exposure at 250°C.

The fundamental reaction mechanism of CZO chemiresistive gas sensor towards several hazardous gases in dry synthetic air can be described by adsorption of interstices oxygen molecules on the sensor surface and direct reaction of them with the analyte gas molecules. It is well documented that the sensing mechanism of ZnO based chemiresistive as sensors is chiefly accredited to the change in electrical resistance due to the adsorption and desorption of analyte gas molecules on the sensor surface. Initially, the oxygen molecules presented in the atmosphere can adsorb on the ZnO surface, extracting the electrons from its conduction band, caused to deteriorate the electron concentration in the conduction band of n-type ZnO semiconductor [23]. As a result, the carrier concentration will decrease so that the initial resistance of the sensor enhanced and the chemisorbed oxygen species like (O^-) may produce on the sensor surface[25]. Furthermore, when CO gas molecules expose on the sensor surface, they react with the oxygen ions and transfer the electrons back into the conduction band of the ZnO layer under the following reaction mechanism[26].

$$O_{2(gas)} \rightarrow 2O_{(adsorbed)} \quad (1)$$

$$O_{(adsorbed)} + e^-_{(from\ ZnO)} \rightarrow O^- \quad (2)$$

$$CO_{(adsorbed)} + O^- \rightarrow CO_2 + e^-_{(to\ ZnO)} \quad (3)$$

Therefore, the resistance of the sensing layer starts to decline. The active sites for oxygen and the analyte gas molecules on the sensor surface is the crucial factor for the improvement of the gas sensing characteristics[27]. In this work, as the oxygen vacancies increase and other defects which are accessible by Cu doping, leading to more active sites for the fast reactions takes place so that the gas sensing properties of ZnO thin films can significantly improve. During the recovery process, the reducing gas molecules extracted out from the sensing chamber so that the number of electron concentration starts to deteriorate which causes to the recover the original electrical signal at the operating temperature of 250°C[28].

Conclusion

The aim of the present work was to synthesize the high quality CZO nanocrystalline thin films on glass substrates by DC magnetron sputtering technique at room temperature and to investigate the effect of Cu doping on structural, morphological and sensing properties to obtain better quality of device. We developed a high sensitive and selective CO gas sensor based on CZO thin film. The sensor depicts a significantly high sensing response towards 50-1000 ppm CO with a fast response and recovery time. The high sensor response, good selectivity, stability and low temperature operation make this sensor appreciable for industrial applications. Therefore, the application of CZO sensor becomes very encouraging for simple and low cost based sensor for detecting the low concentration of CO gas up to several ppm level in our environment.

Acknowledgments

The author Pawan Kumar would like to acknowledge the financial support from the Ministry of Human Resource, India.

References

1. L. Dang, G. Zhang, K. Kan, Y. Lin, F. Bai, L. jing, P. Shen, L. Li, K. Shi, Journal of Materials Chemistry A, 2 (2014) 4558-4565.
2. F. Shao, M.W.G. Hoffmann, J.D. Prades, R. Zamani, J. Arbiol, J.R. Morante, E. Varechkina, M. Rumyantseva, A. Gaskov, I. Giebelhaus, T. Fischer, S. Mathur, F. Hernández-Ramírez, Sensors and Actuators B: Chemical, 181 (2013) 130-135.
3. K. Sircar, J. Clower, M.k. Shin, C. Bailey, M. King, F. Yip, The American Journal of Emergency Medicine, 33 (2015) 1140-1145.
4. A. Sanger, A. Kumar, A. Kumar, J. Jaiswal, R. Chandra, Sensors and Actuators B: Chemical, 236 (2016) 16-26.
5. T. Li, W. Zeng, Z. Wang, Sensors and Actuators B: Chemical, 221 (2015) 1570-1585.
6. Z. Dai, L. Xu, G. Duan, T. Li, H. Zhang, Y. Li, Y. Wang, Y. Wang, W. Cai, Scientific Reports, 3 (2013) 1669.
7. S. Jain, A. Sanger, S. Chauhan, R. Chandra, Materials Research Express, 1 (2014) 035046.
8. A.V. Radhamani, K.M. Shareef, M.S.R. Rao, ACS Applied Materials & Interfaces, 8 (2016) 30531-30542.
9. M. Hjiri, R. Dhahri, L. El Mir, A. Bonavita, N. Donato, S.G. Leonardi, G. Neri, Journal of Alloys and Compounds, 634 (2015) 187-192.
10. A. Sanger, P.K. Jain, Y.K. Mishra, R. Chandra, Sensors and Actuators B: Chemical, 242 (2017) 694-699.
11. C.R. Michel, A.H. Martínez-Preciado, N.L.L. Contreras, Sensors and Actuators B: Chemical, 184 (2013) 8-14.
12. R. Dhahri, M. Hjiri, L. El Mir, H. Alamri, A. Bonavita, D. Iannazzo, S.G. Leonardi, G. Neri, Journal of Science: Advanced Materials and Devices, 2 (2017) 34-40.
13. X.-T. Yin, X.-M. Guo, Sensors and Actuators B: Chemical, 200 (2014) 213-218.
14. A. Kumar, A. Sanger, A. Kumar, R. Chandra, RSC Advances, 6 (2016) 47178-47184.
15. A. Kumar, A. Sanger, A. Kumar, R. Chandra, RSC Advances, 6 (2016) 77636-77643.
16. M.T. Hosseinnejad, M. Ghoranneviss, M.R. Hantehzadeh, E. Darabi, Journal of Alloys and Compounds, 689 (2016) 740-750.
17. Y.-J. Li, K.-M. Li, C.-Y. Wang, C.-I. Kuo, L.-J. Chen, Sensors and Actuators B: Chemical, 161 (2012) 734-739.
18. H. Gong, J.Q. Hu, J.H. Wang, C.H. Ong, F.R. Zhu, Sensors and Actuators B: Chemical, 115 (2006) 247-251.
19. R.K. Shukla, A. Srivastava, N. Kumar, A. Pandey, M. Pandey, Journal of Nanotechnology, 2015 (2015) 10.
20. A. Sanger, A. Kumar, A. Kumar, R. Chandra, Sensors and Actuators B: Chemical, 234 (2016) 8-14.
21. R.M. Geatches, A.V. Chadwick, J.D. Wright, Sensors and Actuators B: Chemical, 4 (1991) 467-472.
22. A. Sanger, A. Kumar, S. Chauhan, Y.K. Gautam, R. Chandra, Sensors and Actuators B: Chemical, 213 (2015) 252-260.
23. X. Deng, L. Zhang, J. Guo, Q. Chen, J. Ma, Materials Research Bulletin, 90 (2017) 170-174.
24. S.-J. Choi, S. Chattopadhyay, J.J. Kim, S.-J. Kim, H.L. Tuller, G.C. Rutledge, I.-D. Kim, Nanoscale, 8 (2016) 9159-9166.
25. C. Xu, S. Chung, M. Kim, D.E. Kim, B. Chon, S. Hong, T. Joo, Journal of Nanoscience and Nanotechnology, 5 (2005) 530-535.
26. C.H. Tan, S.T. Tan, H.B. Lee, R.T. Ginting, H.F. Oleiwi, C.C. Yap, M.H.H. Jumali, M. Yahaya, Sensors and Actuators B: Chemical, 248 (2017) 140-152.
27. T. Sin Tee, T. Chun Hui, C. Wu Yi, Y. Chi Chin, A.A. Umar, G. Riski Titian, L. Hock Beng, L. Kok Sing, M. Yahaya, M.M. Salleh, Sensors and Actuators B: Chemical, 227 (2016) 304-312.
28. H. Gu, Z. Wang, Y. Hu, Sensors, 12 (2012) 5517.

